Electronic Supplementary Information

Recovery and Reuse of Homogeneous Palladium Catalysts via Organic Solvent Nanofiltration: Application in the Synthesis of AZD4625

Hui Xiao,[*a] William R. F. Goundry,[a] Rhys Griffiths,[a] Yanyue Feng[b] and Staffan Karlsson[b]

a Early Chemical Development, Pharmaceutical Sciences, Biopharmaceuticals R&D, AstraZeneca, Macclesfield SK10 2NA, United Kingdom;

b Early Chemical Development, Pharmaceutical Sciences, Biopharmaceuticals R&D, AstraZeneca Gothenburg, SE-431 83 Mölndal, Sweden.

*Email: hui.xiao4@astrazeneca.com

Note S1: Methods of Life Cycle Assessment (LCA).

The LCA involved a cradle-to-gate assessment, encompassing all upstream activities associated with catalyst synthesis, use, and recovery, while omitting further transformation of the reaction products into other compounds.[1] The functional unit here is 1 kg of the limiting material (LM, benzophenone imine). Two processes (membrane and non-membrane process) are compared based on the mass flows from our experimental data. In the non-membrane process, the Pd catalyst is removed by the CUNO filter, meaning the catalyst/ligand cannot be reused. The membrane process assumes the catalyst/ligand are reused for five cycles and 6 DVs of solvents are used in each cycle. To simplify the model, the manufacturing and disposal of the OSN membrane module and CUNO filters were not considered due to lack of data. Additionally, we only compared the two processes based on the global warming potential (GWP) of the catalyst/ligand and solvents. Other starting materials were not considered due to the same amount materials being used in both cases. Thus, our estimates provide a lower bound on the true impact that would result from a more detailed LCA when more accurate data become available.

The GWP for each process was derived from the following equation:

$$GWP_{process} = {CO_2e}_{Process} = \sum\left(m_{input,i}\frac{{CO_2e}_{Raw\ Material\ Production,i}}{kg\ i}\right) + m_{solvent\ waste}\frac{{CO_2e}_{S}}{kg} - m_{Pd\ available\ for\ recovery}\frac{{CO_2e}_{Pd\ Production}}{kg\ Pd}$$

The first term on the right-hand-side of this equation is the contribution due to the production of raw materials used in the reaction process. Where i = Xantphos, $Pd(dba)_2$ and 2-MeTHF. Reactants and work-up materials were not considered in this calculation as they are equivalent between the two processes. The second term on the right-hand-side of this equation is the contribution due to the direct emissions (degradation) from solvent incineration. It does not consider emissions due to machinery operation or transportation. The third term on the right-hand-side of this equation is the potential savings associated with the recovery of palladium metal in the final retentate stream or within the CUNO filter. This is considered as a carbon saving, equivalent to the reduction in emissions from avoiding the extraction and refining of additional palladium ore and metal. Due to insufficient data, this does not consider transportation of palladium-rich waste streams, nor does it consider the operating emissions of the palladium recovery process. A solvent recycling ratio was manipulated within the mass balance boundary to affect the quantities of fresh 2-MeTHF required by the membrane process, as well as the quantity of solvent waste.

The difference between the membrane and non-membrane process were then subtracted from each other to give the difference between the two processes:

$$\Delta\frac{GWP}{kg\ LM} = \frac{GWP_{\ Membrane}}{kg\ LM} - \frac{GWP_{Fresh\ Catalyst}}{kg\ LM}$$

All the GWP data are from ecoinvent v3.5. The GWP of $Pd(dba)_2$ is 3040 kg CO_2e/kg, and the GWP of Pd metal is 11054 kg CO_2e/kg. However, due to the lack of data, for petroleum-derived 2-MeTHF, we use the data for THF as an approximate (7.7 kg CO_2e/kg). The incineration of petroleum-derived 2-MeTHF incurs a GWP of 2.69 kg CO_2e/kg. The GWP of bio-derived 2-MeTHF is 3.24 kg CO_2e/kg, adapted from the literature[2] for the manufacturing of 2-MeTHF from bagasse, with the impact of waste treatment assumed to be zero. For the GWP of Xantphos, we used the data for X-phos as an approximate (203 kg CO_2e/kg).

In the base case (Scenario 1), petroleum-derived 2-MeTHF is used for both processes, and no Pd recovery/refining and solvent recycling is considered. Scenario 2 refers to the base case but uses bio-derived 2-MeTHF to replace petroleum-derived 2-MeTHF. Scenario 3 also refers to the base case, but a Pd catalyst recovery and refining process is added (Fig. S1a and b). This 80% of recovery efficiency is estimated by considering both the collection efficiency (10-20% Pd lost during the extractive work up) and Pd recovery efficiency (90%). The Pd recovery process mainly affects the non-membrane process, due to the membrane process can reuse the catalyst and the residue of Pd after 5th batches is only about 20%. Scenario 4 refers to the base case, but both the catalyst recovery and solvent recycling are added (Fig. S1c). For simplification, carbon emissions related to Pd catalyst recovery and solvent recycling were not considered. The solvent recycling of the diafiltration solvent for the membrane process can greatly reduce the solvent consumption. The limit of the solvent recycling is ~95%, considering the solubility of the product (300 mg/mL). The detailed calculated results are presented in Table S1.

We also calculated the solvent consumption, process mass intensity and E-factor of the membrane process with and without the integration of solvent recycling units in Table S2.

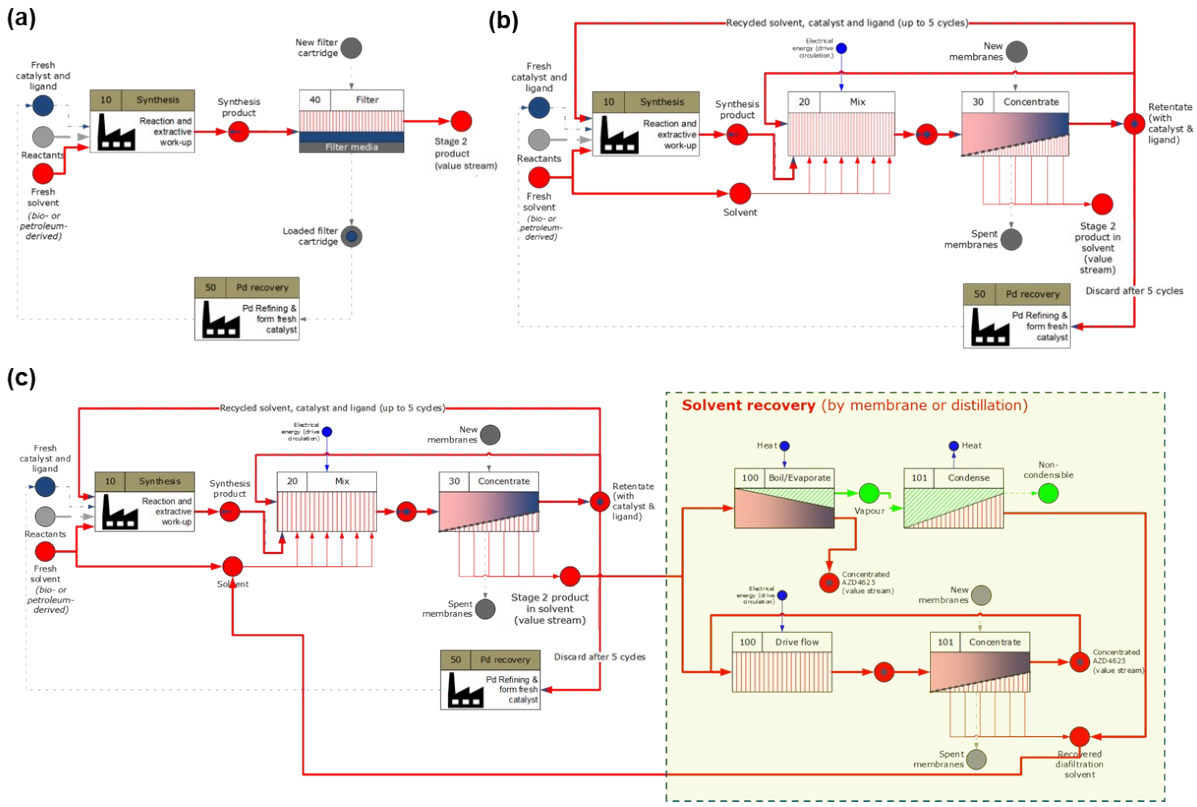

Fig. S1 Process scheme of (a) non-membrane process with catalyst recovery, (b) membrane process with catalyst recovery, and (c) membrane process with catalyst recovery and potential solvent recovery by membrane or distillation.

Table S1 GWP comparison of the membrane process and non-membrane process in Scenario 1-4.

GWP (kg CO2/ kg LMs)	Scenario 1 : Petroleum-based 2-MeTHF		Scenario 2: Scenario 1 + bio-derived 2-MeTHF		Scenario 3: Scenario 1 + catalyst recovery		Scenario 4: Scenario 1 + catalyst recovery/solvent recycling	
	Non-membrane process	Membrane process	Non-membrane process	Membrane process	Non-membrane process	Membrane process	Non-membrane process	Membrane process
2MeTHF	101.2	405.0	42.6	170.4	101.2	405.0	101.2	38.2
$Pd(dba)_2$	144.7	28.9	144.7	28.9	144.7	28.9	144.7	28.9
Xantphos	13.0	2.6	13.0	2.6	13.0	2.6	13.0	2.6
Incinaration of 2MeTHF	27.1	133.2	0.0	0.0	27.1	133.2	27.1	0.5
Catalyst recovery	0.0	0.0	0.0	0.0	-77.9	-3.1	-77.9	-3.1
Sum	286.0	569.7	200.2	201.9	208.1	566.6	208.1	67.0

Table S2 Summary of solvent consumption, process mass density and E-factors for both membrane and non-membrane process

Green Metric	Non-membrane Process	Membrane Process (No solvent recycling)	Membrane Process (Max solvent recycling)
Solvent Consumption (kg / kg LMs)	13.1	52.6	4.8
Solvent Consumption (L / kg LMs)	15.5	61.9	5.6
Process Mass Intensity (kg input / kg product)	31.9	69.5	25.4
E-Factor (kg waste / kg product)	30.9	68.5	24.4

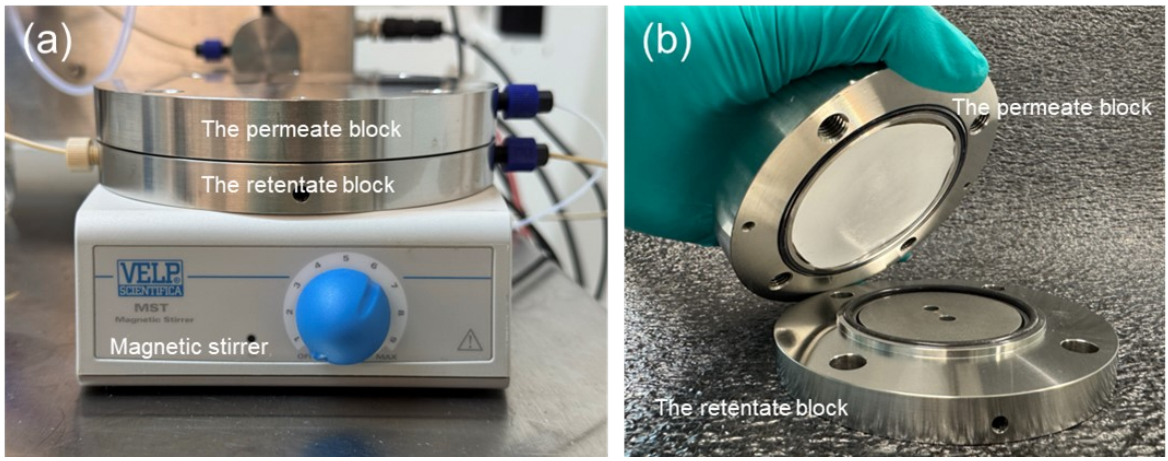

Fig. S2 Structure of the membrane cell used for membrane filtration experiments: (a) Overview of the membrane cell on a magnetic stirrer. The bottom section serves as the retentate block, while the top section serves as the permeate block. (b) Inner structure of the membrane cell. A Φ75 mm membrane filter is assembled on top of a permeate spacer within the permeate block, while a magnetic stirrer bar is fitted inside the retentate block.

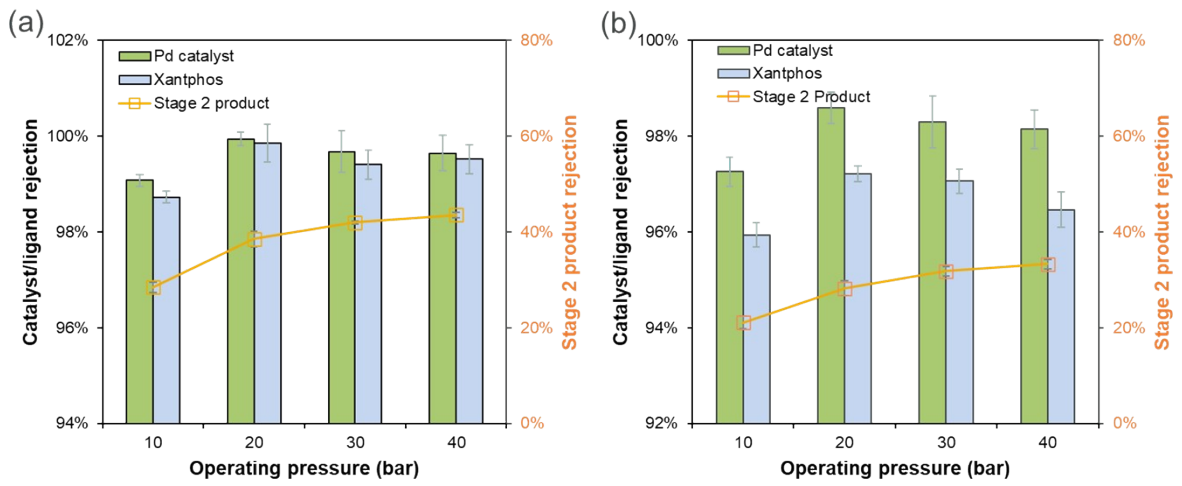

Fig. S3 Operating pressure effect on membrane rejection (a) Borsig oNF-1 (600 Da) and (b) Borsig oNF-2 (350 Da).

Table S3 Detailed data for membrane permeance and rejection towards the catalyst, ligand, and product.

Entry	Membrane type	Trial	Permeance (L m^{-2} h^{-1} bar^{-1})	$Pd(dba)_2$ rejection	Xantphos rejection	Stage 1 product rejection	Stage 2 product rejection
1	Borsig oNF-1	-	3.9 ± 0.07	100 ± 0.1%	99.6 ± 0.3%	82.8 ± 1.0%	38.6 ± 1.6%
		1	3.88	99.78%	100.00%	82.24%	36.71%
		2	3.92	100.00%	99.63%	83.80%	39.74%
		3	4.02	100.00%	99.43%	81.99%	39.22%
2	Borsig oNF-2	-	4.3 ± 0.2	98.5 ± 0.2%	97.2 ± 0.4%	59.4 ± 0.9%	28.3 ± 2.5%
		1	4.08	98.60%	97.60%	59.38%	30.72%
		2	4.51	98.71%	97.22%	61.21%	25.79%
		3	4.2	98.23%	96.88%	60.37%	28.30%
3	Borsig oNF-3	-	9.5 ± 0.9	95.1 ± 0.5%	91 ± 0.5%	48.5 ± 1.0%	-
		1	9.17	94.56%	90.97%	49.54%	
		2	8.86	95.15%	93.55%	48.45%	
		3	10.5	95.48%	92.56%	47.56%	
4	Evonik Puramem® Selective	-	0.7 ± 0.01	96.9 ± 0.5%	97 ± 0.8%	89.1 ± 0.9%	-
		1	0.69	96.31%	97.04%	89.14%	
		2	0.69	96.88%	96.20%	88.33%	
		3	0.68	97.38%	97.76%	90.03%	
5	Evonik Puramem® Performance	-	1.8 ± 0.02	98.3 ± 0.3%	97.3 ± 0.5%	89.3 ± 0.8%	56.3 ± 1.0%
		1	1.83	98.34%	97.32%	89.35%	55.21%
		2	1.79	98.04%	96.80%	88.54%	57.19%
		3	1.80	98.63%	97.77%	90.16%	56.40%
6	Evonik Puramem® Flux	-	6.9 ± 0.1	96.5 ± 0.6%	95.5 ± 0.8%	63.7 ± 0.7%	-
		1	6.92	96.46%	95.89%	63.60%	
		2	6.80	96.88%	96.01%	64.46%	
		3	7.00	95.76%	94.65%	63.12%	
7	Solsep NF10206	-	0.9 ± 0.09	93.2 ± 0.3%	92.9 ± 0.3%	92.5 ± 0.3%	-
		1	0.85	93.05%	92.89%	92.60%	
		2	0.92	93.49%	93.18%	92.75%	
		3	1.02	92.96%	92.63%	92.23%	

Table S4 Conversion, product recovery, and catalyst retention in each reaction cycle using Borsig oNF-2 (350 Da).

Cycle	Conversion in 24 h (%)	Product recovery after 5 DV (%)	Catalyst retention (%)	Ligand retention (%)
1	98.3	97.2	90.4	85.2
2	98.4	97.5	86.9	85.0
3	96.4	97.2	91.9	93.6
4	90.0	97.6	90.0	95.9
5	20.1			

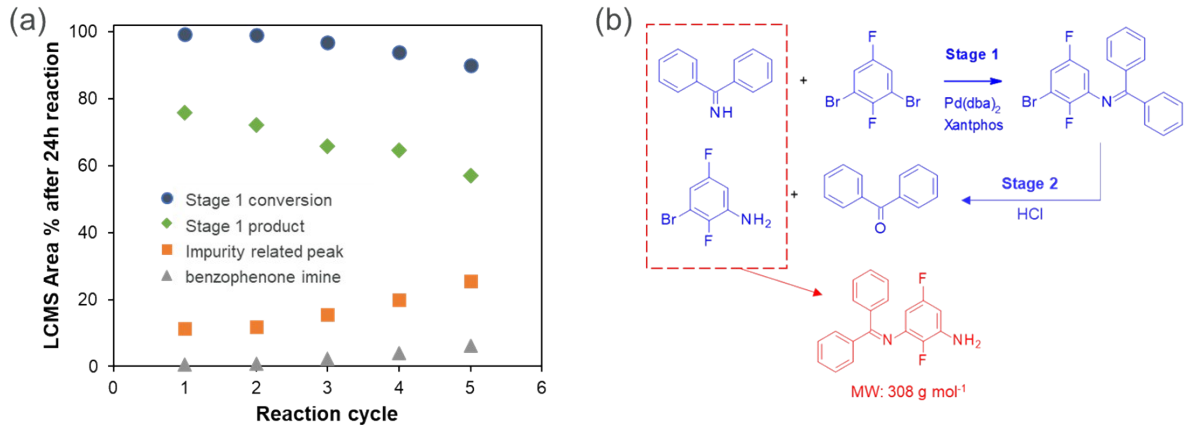

Fig. S4 (a) Area% in HPLC-MS curves after 24 hours of Stage 1 reaction over successive reaction cycles. The impurity related peak overlaps with the peak of the dba ligand in $Pd(dba)_2$. However, it shows a gradual increase with the reaction cycles, indicating the accumulation of the impurity. (b) Possible side reaction related to the formation of the impurity with a molecular weight of 308 g mol^{-1} detected in the HPLC-MS. The reaction occurs between the Stage 2 product (1-2% residue in the recovered catalysts after diafiltration) and the Stage 1 starting material of benzophenone imine.

Note S2: Catalyst degradation.

Catalyst degradation may also happen during the diafiltration process, due to the exposure of the reaction mixture to air. To further investigate whether the catalyst oxidizes significantly during diafiltration, we used ^{31}P NMR to measure the catalyst species in dimethyl sulfoxide (DMSO). The ^{31}P NMR spectra were recorded on a Bruker A400 spectrometer operating at 161.98 MHz for phosphorus nuclei at room temperature. Samples were prepared by dissolving in deuterated DMSO-d_6.

In this experiment, a mixture of $Pd(dba)_2$ and Xantphos (mole ratio 1:1.33) in 2-MeTHF was divided into two group. One group was stirred in air, while the other group contained a piece of the Borsig oNF-1 membrane immersed in the solution and was also stirred in air. Fig. S5 shows the ^{31}P NMR results for the $Pd(dba)_2$/Xantphos complex in the air with time. The peak pairs at -22.9 ppm and +24.5 ppm correspond to Xantphos mono-oxide, while the peak at +25.5 ppm is attributed to Xantphos bis-oxide.[3] This clearly demonstrates that over time, Xantphos undergoes oxidation to form Xantphos mono-oxide, which is further oxidized to Xantphos bis-oxide.

To quantify catalyst degradation over time, we summarized the ratio of the main peak, which corresponds to the unoxidized catalyst (Pd(dba)Xantphos), in Table S5. The results showed a gradual decrease in the ratio of unoxidized catalyst with time for both samples. Importantly, there was no significant difference between the solution containing the membrane and the solution without the membrane, indicating that the degradation process is not related to the membrane itself.

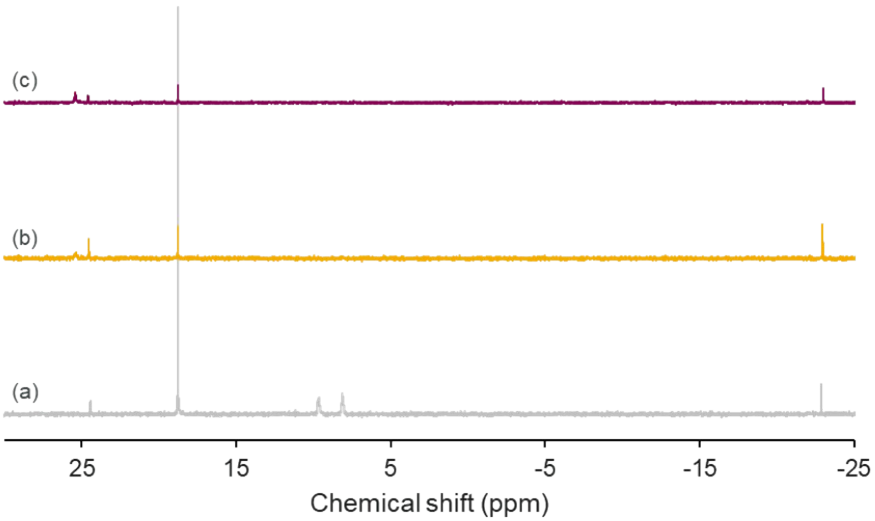

Fig. S5 ^{31}P NMR spectra for the $Pd(dba)_2$/Xantphos sample stirred in the air (a) 0 h, (b) 23 h and (c) 42 h.

Table S5 ^{31}P NMR results for the catalyst degradation.

Time/h	unoxidized catalyst ratio (in air)	unoxidized catalyst ratio (in air with membrane)
0	55.3 ± 2.1%	55.3 ± 2.1%
23	29.7 ± 2.8%	32.3 ± 2.5%
42	19.2 ± 1.6%	21.9 ± 2.0%

Note S3: The purity of the product after diafiltration.

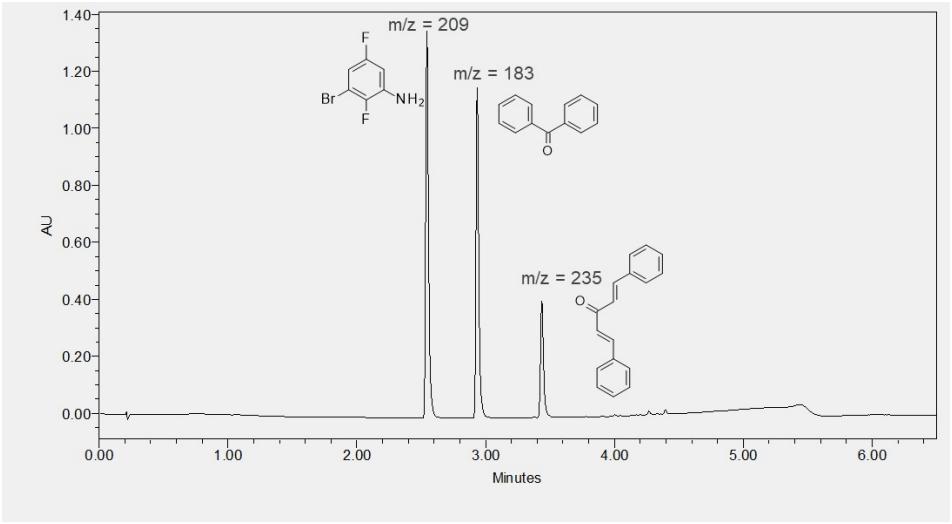

Fig. S6 HPLC-MS spectrum of the permeate solution after the 1st diafiltration with Borsig oNF-1 membrane. Three main peaks based on the MS data corresponds to the main product (mono-bromo-difluoro aniline), the by-product benzophenone and the dba ligand, respectively.

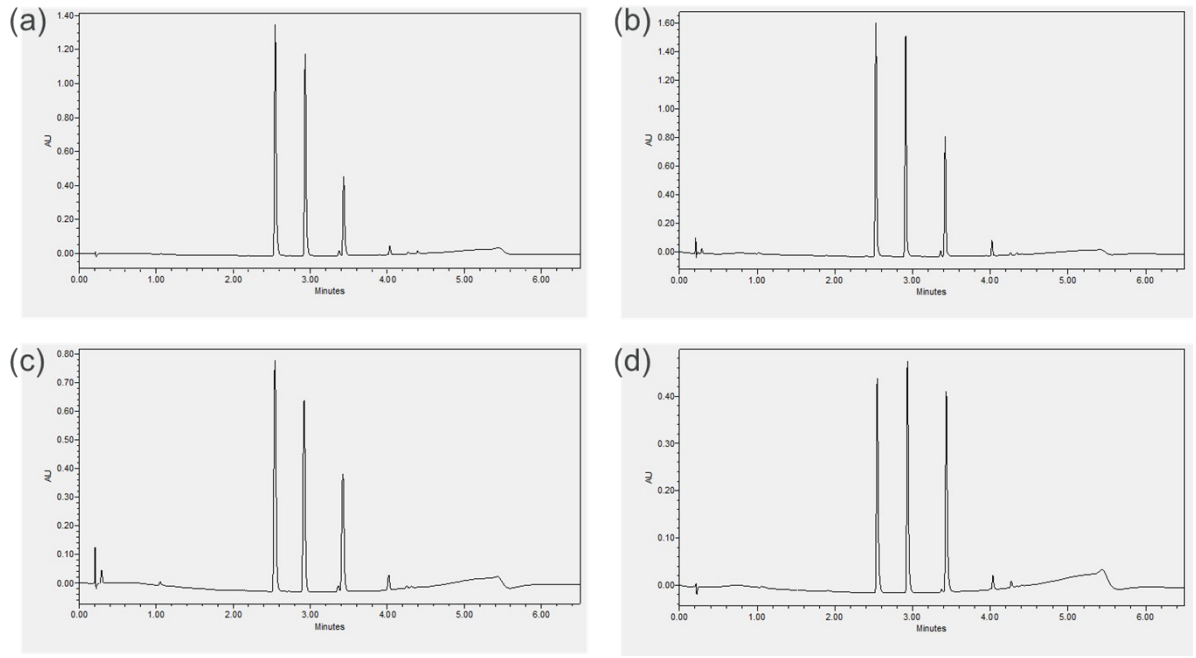

Fig. S7 HPLC-MS spectra of the permeate solution after (a) the 2nd diafiltration (b) the 3rd diafiltration (c) the 4th diafiltration and (d) 5th diafiltration with Borsig oNF-1 membrane.

Table S6 the Pd content relative to Stage 2 product in the permeate after each diafiltration experiment using oNF-1 membrane.

Cycle	Pd content (μg Pd /g product)
1	484
2	561
3	606
4	757
5	765

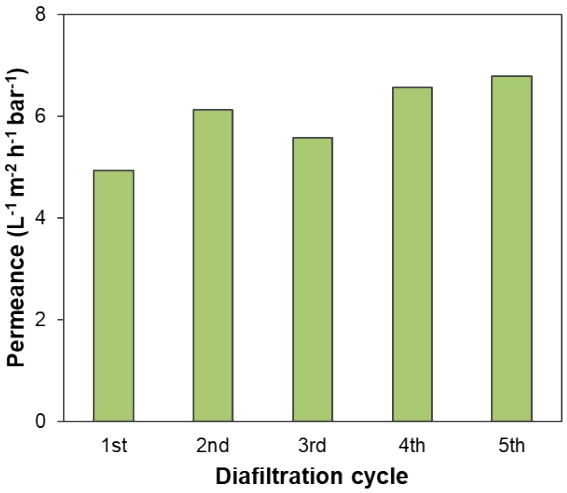

Fig. S8 Membrane permeance (Borsig oNF-1) in the pure 2-MeTHF, before each diafiltration cycle, during the catalyst reuse experiments.

Table S7 Catalyst, ligand and catalyst/ligand rejections by Borsig oNF-1-600Da.

Chemicals	Pd rejection	P rejection
$Pd(dba)_2$	99.9% ± 0.2%	-
Xantphos	-	98.7% ± 0.4%
$Pd(dba)_2$/Xantphos	100% ± 0.1%	99.4% ± 0.3%

Supplementary References

1. D. Faust Akl, D. Poier, S. C. D'Angelo, T. P. Araújo, V. Tulus, O. V. Safonova, S. Mitchell, R. Marti, G. Guillén-Gosálbez and J. Pérez-Ramírez, *Green Chem.*, 2022, **24**, 6879-6888.
2. N. Leroy-Parmentier, P. Loubet, M. Saint-Jean, N. Patouillard and G. Sonnemann, *ACS Sustainable Resource Management*, 2024, **1**, 1548-1562.
3. Y. Ji, R. E. Plata, C. S. Regens, M. Hay, M. Schmidt, T. Razler, Y. Qiu, P. Geng, Y. Hsiao, T. Rosner, M. D. Eastgate and D. G. Blackmond, *J. Am. Chem. Soc*., 2015, 137, 13272-13281.